ISBN: 978-984-34-8313-3
www.iabse-bd.org

Numerical study of CFRP-strengthened stainless steel sections subjected to web crippling in bridges constriction

S.M.Z. Islam & B. Ahmed
Rajshahi University of Engineering and Technology, Rajshahi 6204, Bangladesh

M.R. Hasan
Bangladesh Army University of Engineering and Technology, Natore, Bangladesh

B. Young
The University of Hong Kong, Hong Kong, China

H.I. Tusher & S. Alam
Rajshahi University of Engineering and Technology, Rajshahi 6204, Bangladesh

ABSTRACT: In bridge construction, the advanced use of stainless-steel is urging day by day for its better structural performance and outstanding features of aesthetics, corrosion resistance, high strength and long-term durability. Recently, Hong Kong-Zhuhai-Macao Bridge (55km), Stone Cutter Bridge in Hong Kong is constructed using the structural benefits of stainless steel. Current available design guidelines very conservative to measure the structural capacity of strengthened stainless-steel sections imperiled to web crippling. Numerical simulation model has been paid high attention to overcome laboratory issues in terms of the testing cost and testing time to propose a new wide-ranging design guideline. In this study, series of test has been conducted to propose a finite element model. Tests were performed by considering four different testing conditions specified in the ASCE specification. Geometrical and material non-linear FEA model was proposed for simulating experimental conditions. Total 170 data including 66 test results and 104 simulated FEM data were used for developing design equation. Non-linear cohesive zone modeling and deboning mechanisms are explained using the traction separation laws. From the simulated results, it is observed that the ultimate capacity, failure modes of web-crippling and web deformations were simulated properly. Extensive parametric analysis has been performed by the verified FEM analysis considering different tubular steel sections in different loading conditions. Based on the parametric analysis, a design equation has been established and this design equation results show the excellent agreement of numerical and experimental data. The proposed design equation shows the more accurate and versatile results for strength of web crippling of CFRP enhancement stainless-steel hollow sections.

1 INTRODUCTION

Stainless-steel has high strength capacity and significant corrosion resistance when it is used as structural elements in bridge construction. It has also high durability and it is expanding for applications in bridge construction. Recently, Hong Kong-Zhuhai-Macao Bridge (55kM), Stone Cutter Bridge in Hong Kong bridges and Cala Galdana Road Bridge, Spain has been constructed with stainless-steel as shown in Figure 1.Gedge (2005, 2007, 2008) explained the use of stainless-steel in bridge construction in his research. Structural applications of stainless-steel have been significantly increased since 2000. Twenty bridges since 1999 to 2011 those are constructed by stainless-steel described by Islam and Young (2015). The durability of the stainless-steel bridges is higher than other types of bridges. Such as, Hong Kong-Zhuhai-Macao Bridge (55kM) did not require any maintenance in 120 years. So, stainless-steel bridge is cost effective compared to carbon steel bridges.

Carbon steel bridge has huge structural deficiency during service period and repair, or rehabilitation is required using advanced composite materials. These materials offer an effective result for momentary retrofit or long-term rehabilitation (Miller et al. 2001). FRP materials are used for strengthening purposes for carbon steel bridges which is stated by Tani et al. 2000; Miller et al. 2001; Sen et al. 2001; Katsuyoshi et al. 2005; Suzuki 2005; Schnerch and Rizkalla 2008. The stiffeners used in the bridges those can resist the cripple of the webs of cold-formed stainless steel. Conventionally, the repair works have done by adding external plate and or replace the plates (Zhao and Zhang 2007). However, the existing repairing methods increase the weight of the structures and sometimes it is tough to fix the plates. During repairing works, corrosion risk can be happened, and fatigue comes out of the steel plates. Therefore, externally bonded FRP strengthening practice is the best alternative way to strengthen the structures subjected to load concentration. However, few studies have been done on FRP strengthening of stainless-steel sections in past. Particularly, stainless-steel sections subjected to web crippling have not been investigated properly. Extensive research has to be done for better understanding the structural behaviour of strengthening of stainless steel tubular section subjected to load concentration. Islam and Young (2012, 2014) performed a series of tests for the CFRP strengthened structural elements. All tests were conducted for cold-formed members subjected to web crippling. From the experimental results it is clearly indicated that the ultimate capacity of CFRP strengthened member's increases significantly. In the literature, different numerical simulation works have been found CFRP strengthened members (Islam 2012; Islam and Young 2019).

Currently, 3D numerical tool ABAQUS is used widely to measure the actual behaviour of CFRP strengthened elements. Many design codes such as ASCE, AS/NZ and EN developed for cold-formed stainless-steel members and all these codes have some limitations on material strengths. Design guidelines of bared carbon steel subjected to web crippling by EN code is not applicable for CFRP strengthened structural members. So, there is strong need to propose a unified and new design model to predict the ultimate capacity of CFRP strengthened structural members.

To address the above issues, three different steps have been completed. Firstly, the numerical simulation has been conducted for CFRP strengthened structural members by ABAQUS 2009. Secondly, extensive parametric study has been done for different web slenderness ratio. The value selected for this parametric study ranges from 4.8 to 113.6. Finally, the design guideline is proposed for CFRP strengthened members based on the parametric analysis. The proposed design guideline has been verified by the reliability analysis.

(a) Hong Kong-Zhuhai-Macao Bridge (55kM) (b) Stone cutter bridge, Hong Kong, 2010 (c) Cala Galdana Road Bridge, Spain 2005

Figure 1. Application of stainless-steel in bridge construction.

2 EXPERIMENTAL INVESTIGATIONS

In this study, total 66 specimens were prepared for testing under web crippling. In total 34 specimens were made by ferritic stainless steel and other 32 specimens were by lean duplex stainless steel. All specimens were tested under different loading conditions such as ETF, ITF, EOF and IOF(Islam and Young 2012, 2014). Two types of cross-sections including square and rectangular hollow sections were considered is presented in Figure 2.

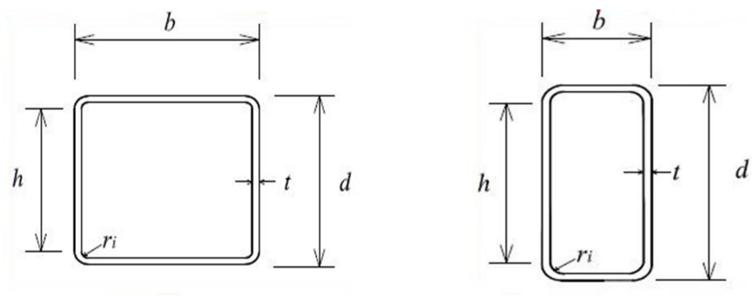

(a) Square tubular steel section (SHS) (b) Rectangular tubular steel section (RHS)

Figure 2. Different types of tubular steel section.

Total 5 ferritic and 5 lean duplex sections were considered for the test under web crippling. The main parameters such as tube thickness range from 1.5 mm to 4 mm and depth of section web varies from 30 mm to 150 mm. The flange width and the web slenderness vary from 30 mm to 150mm and 8.1 to 57.3 respectively. The bearing length was constant for loading configurations (ETF, ITF and IOF) and the constant value was 50mm. The bearing length was different for EOF and the constant value used as 30 mm.

Coupon test was performed to measure material properties. The test was performed by following the instructions of ASTM (1997) and AS (1991) codes(Islam and Young (2012, 2014). Six specimens were denoted by ‘a’ to ‘f’ for FRP and ‘A’ to ‘F’ for adhesive. The important properties of strengthen materials and adhesive were tested by Islam and Young (2012, 2014). Figure 3 illustrated the stress-strain diagram of stainless steel and FRP material. The composition of the composite strengthening materials was determined based on the Islam and Young 2012, 2014model. Before strengthening, the surface treatment is crucial for better performance of strengthening materials. For ferritic steel sections, the surface was treated by sander method is appropriate to achieve the improved results of ultimate capacity. On the other hand, electric grinder surface treatment can perform for the lean duplex tubular sections (Islam and Young 2012, 2014). Section geometry, material properties, number of FRP layer and loading condition was considered according to Islam and Young 2012, 2014 previous article.

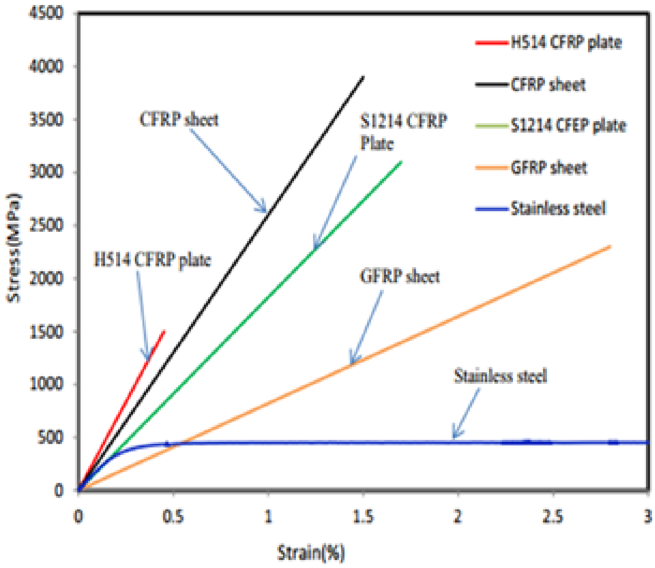

Figure 3. Material properties (σ-ε curve) of steel and strengthening materials.

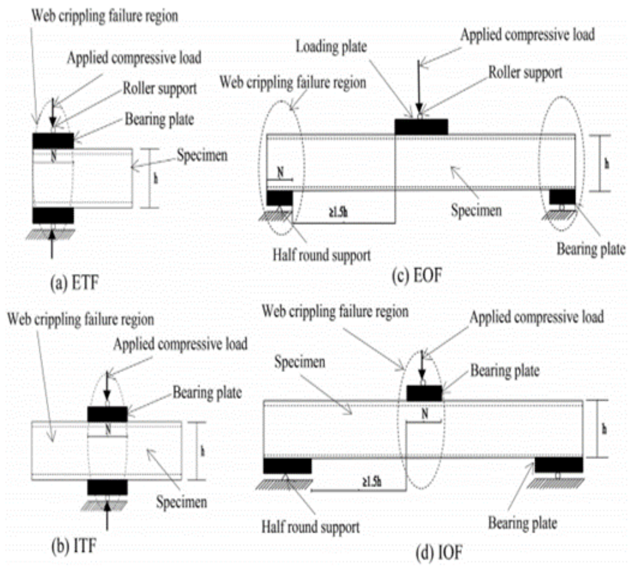

Figure 4. Different loading conditions for web crippling.

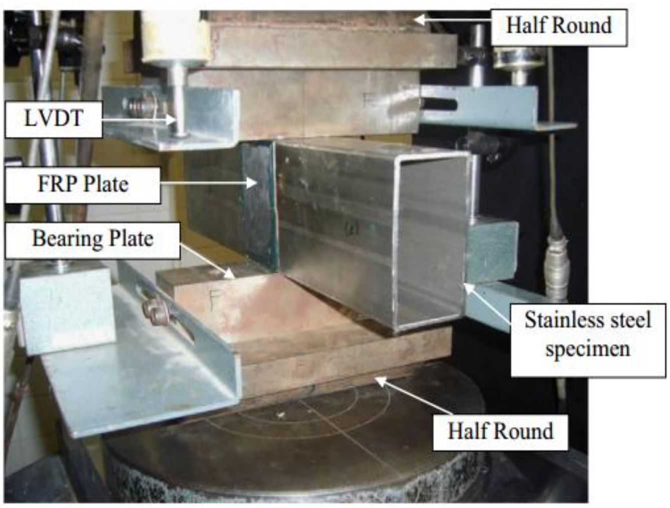

Figure 5. Test set up of ITF loading condition.

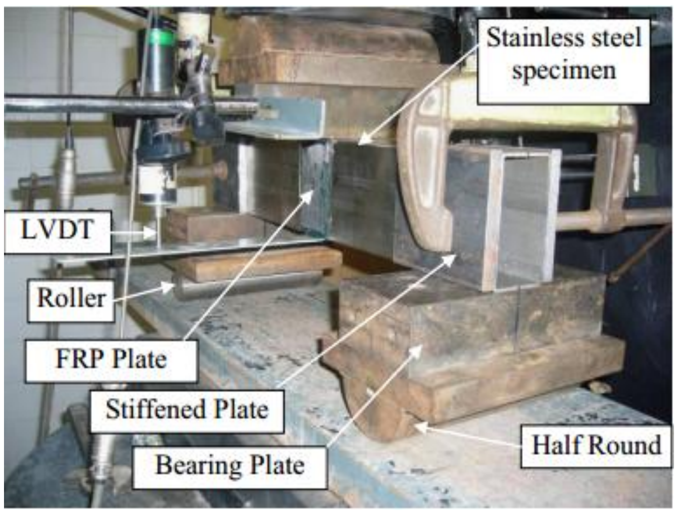

Figure 6. Test set up of IOF loading condition.

Different testing configurations (ETF, ITF, EOF and IOF)are presented in Figure 4. INSTRON servo-controlled hydraulic testing machine was used to conduct the web crippling test of stainless-steel tubular sections. Figure 5-6 shows the testing setup view of ITF and IOF loading conditions. Experimentally, the failure patterns of CFRP strengthened specimen were detected (Islam and Young 2012, 2014). The outward buckling of web has been noticed and it is found that the plastic hinge zone found at ultimate limit state.

3 NUMERICAL ANALYSIS

3.1 *Modelling Descriptions*

Commercially available numerical software ABAQUS (2009) have been used to simulate the test results. To simulate the test results accurately, finite element (FE) modelling was develop for five key parameters. The bearing plates, stainless tubular section, adhesive, CFRP and the interfaces between stainless steel and adhesive were modelled by ABAQUS (2009). In FE modelling 4-node S4R element was considered for the steel section. To avoid the convergence problem and reduce the computational time appropriate mesh size 2mm along the transverse direction and 10mm along the length was used. At the corner of the section, comparatively smaller mesh size was used as shown in Figure 7. The boundary conditions were restrained along the vertical axis.

For the steel bearing plate, C3D8R solid element was considered. The interaction between stainless section and bearing plate was considered as “contact pair”. Geometrical non-linearity (*NLGEOM) was considered for the analysis. Displacement was applied as load and static general loading method was considered. Actual testing configuration was made in FEA to capture the actual behaviour. For the FE analysis certain displacement 5mm was applied as load. The FE modelling procedure details are given in Islam and young (2018).

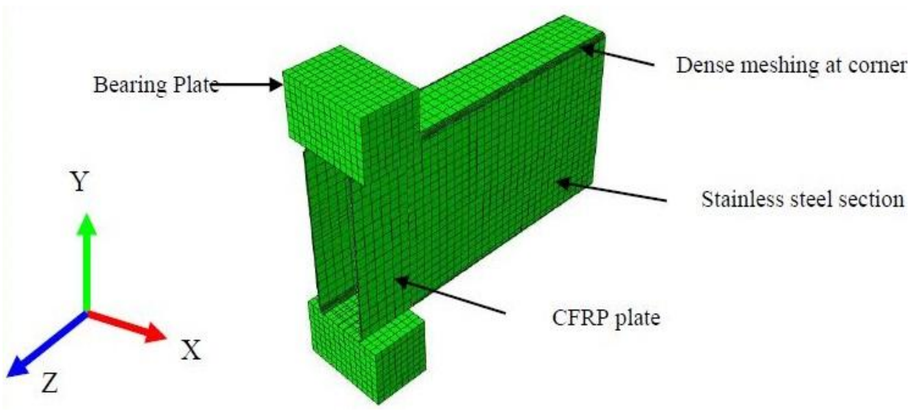

Figure 7. FE modelling and meshing of stainless-steel section and bearing plate.

3.2 *Material Model*

From the coupon test, the material model of stainless-steel tube was developed. Multi-linear stress-strain curve prepared from regression analysis. The true stress was calculated from the engineering stress and the conversion has been performed based on Eq. (1). Similarly, the true strain also calculated from the engineering strain according to Eq. (2). Plastic true strain has been used in ABAQUS model. The plastic true strain is related to true stresses and logarithmic strains. The Eq. (3) is shown to calculate the true plastic strain.

$$\sigma_{true} = \sigma(1+\varepsilon) \quad (1)$$

$$\varepsilon_{true} = ln(1+\varepsilon) \quad (2)$$

$$\varepsilon_{true}^{pl} = ln(1+\varepsilon) - \sigma_{true}/E_0 \quad (3)$$

where, $E_{o,}$ σ and ε are initial modulus of elasticity, engineering stress and strain respectively. The elastic modulus of CFRP was taken as 210-300 GPa and thickness 1.4 mm. S4R elements was used for CFRP material in FE modelling. Poisson’s ratio was taken as 0.33.Cohesive COH3D8 element was considered for the adhesive material. The debonding between steel surface and epoxy resin is explained by traction-separation law.

4 FE MODEL VERIFICATION

The experimental results were simulated by the FE model. The ultimate capacity, deflection, web-buckling and the failure modes were calibrated by FE analysis. In Figure 8, the failure modes obtained from test results and FE analysis of square and rectangular specimens are illustrated. The full range curves of tested results at different loading configurations are verified by FE analysis and very good agreement has been found is shown in Figure 9-12. In particular, the prediction of ultimate capacity with respect to slenderness ratio for ETF and ITF loading configuration is shown in Figure 13. Excellent agreement has been attained between the FE simulations results (P_{uc}) and the measured test values (P_{ue}) for both ferritic duplex steel sections.

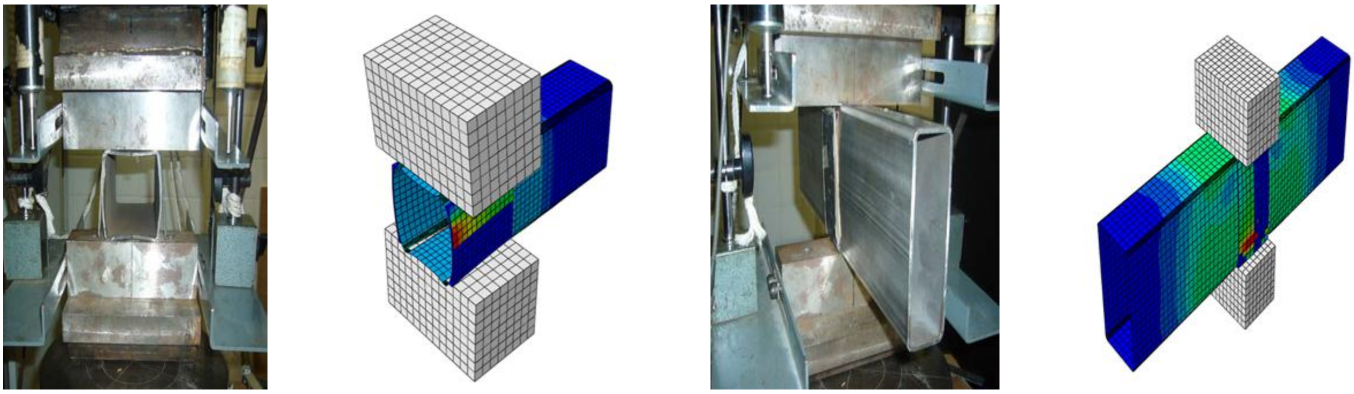

(a) Experimental (b) FEA (c) Experimental (d) FEA

Figure 8. Failure modes and debonding of specimen in test and FE analysis.

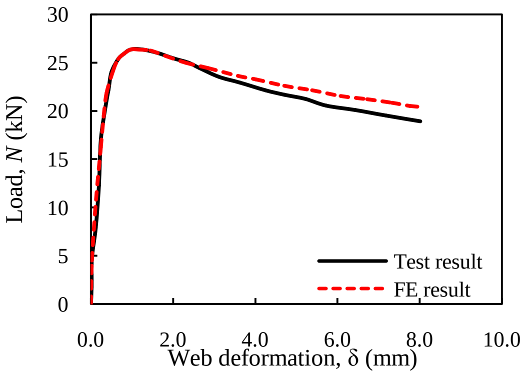

Figure 9. Load-web deformation comparison under ETF loading.

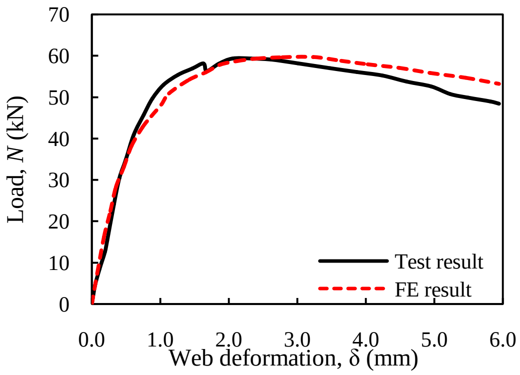

Figure 10. Load-web deformation comparison under ITF loading.

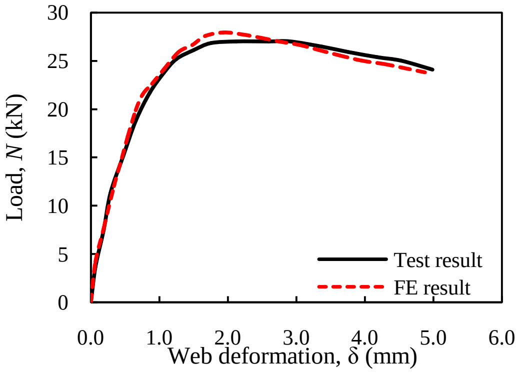

Figure 11. Load-web deformation comparison under EOF loading.

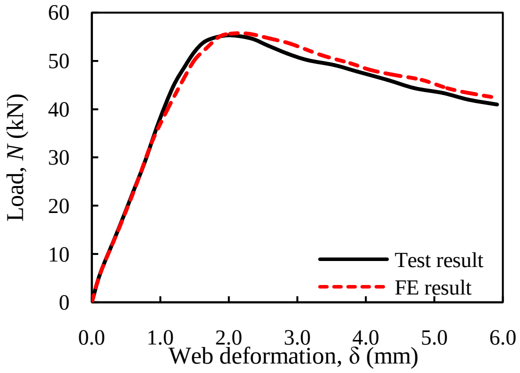

Figure 12. Load-web deformation comparison under IOF loading.

The overall mean (μ_m) and coefficient of variance (COV) of predicted results is 1.03 and 0.041 for ferric stainless-steel sections and 1.02 and 0.034 for duplex stainless-steel sections.

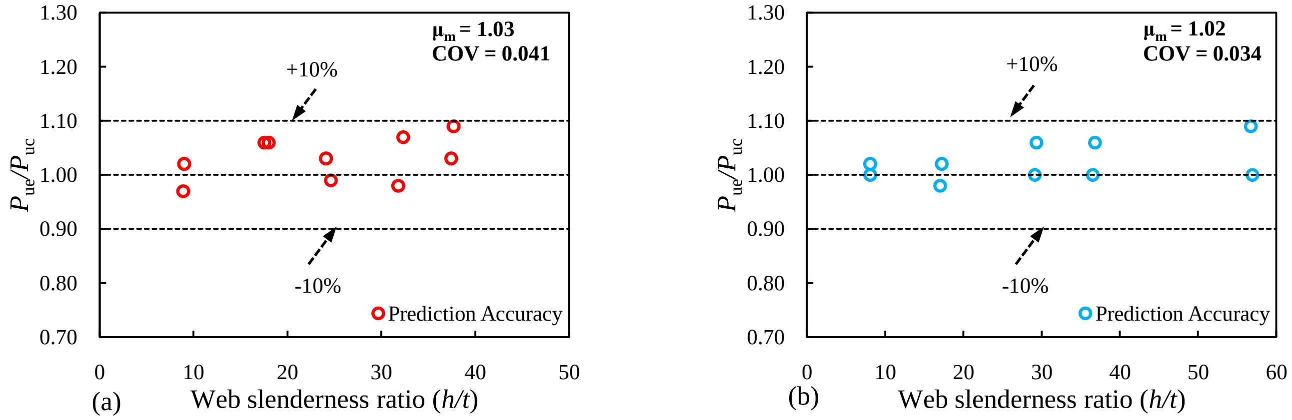

Figure 13. Predicted strength by FEM under a) ETF loading condition for ferritic and b) ITF loading for duplex section.

5 PARAMETRIC STUDY

Extensive parametric study has been done to figure out the effect physical parameters. Different controlling key parameters such as cross-section of tube, thickness of steel tube, and web slenderness ratio (*h/t*) were taken for the study. FE analysis has been performed for 104 specimens. 48 specimens for ferritic steel sections and 56 duplex steel specimens were considered. Two different types of sections including square and rectangular sections were selected for both ferritic and lean duplex sections. The prediction of the ultimate capacity for ETF and ITF loading condition from the parametric study with respect to slenderness ration is shown in Figure 14. From the results it is showed that the overall mean (μ_m) and coefficient of variance is 1.05 and 0.155 respectively. It shows good agreement with the FE or test results. From the parametric study it can be concluded that the slenderness ration rises to 66.6 and 71.0 for lean duplex steel and ferritic section for CFRP strengthening. This ratio demonstrated the most favourable condition for CFRP strengthening. The strength of CFRP strengthening section increases until a certain limit for slenderness ratio.

6 RELIABILITY INDEX PARAMETER

The accuracy of the proposed design formula is rectified by reliability index parameter. Reliability index is denoted by β. The web crippling design was proposed, and the formula is rectified by the safety factors in this study. The lower limit of the reliability index is 3.0 according to existing design code ASCE for stainless steel. In this study, the design equation was accepted for the reliability index of greater than 2.5. The combination of total load was measured by the ASCE code for reliability analysis. The load combination is done by dead load (DL) and live load (LL) and the load combination is 1.2DL+1.6LL. In total 170 results including 66 test results and 104 simulation results were taken for the reliability analysis. Statistical parameters range as M_m = 1.10, F_m = 1.00, V_M = 0.10, and V_F = 0.05 were used according to NAS specification. Mm, Fm, V_M and V_F denoted as mean values and coefficients of variation for material properties and fabrication variables. The mean and coefficient variance of the predicted design strength found as 1.05, 0.155 and 1.03, 0.123 respectively for ferric and duplex stainless-steel section.

7 PROPOSED DESIGN EQUATION (P_P)

Professional engineers are always eager to find the accurate practical design guidelines for CFRP strengthened steel sections. Available existing design codes are not always show the better performance for predicting the design strength for CFRP strengthened steel sections. Unique design formula has been developed for CFRP strengthened steel sections under for specified loading conditions.

Considering the influence of the all controlling parameters of steel, CFRP and adhesive materials, design Eq. (4) has been proposed. From the parametric analysis, new co-efficient of C, C_N, Ch and $C_{ad\text{-}CFRP}$ shown in Table 1 for both types of seel sections. The new design formula developed based on parametric analysis is shown in Eq. 4.

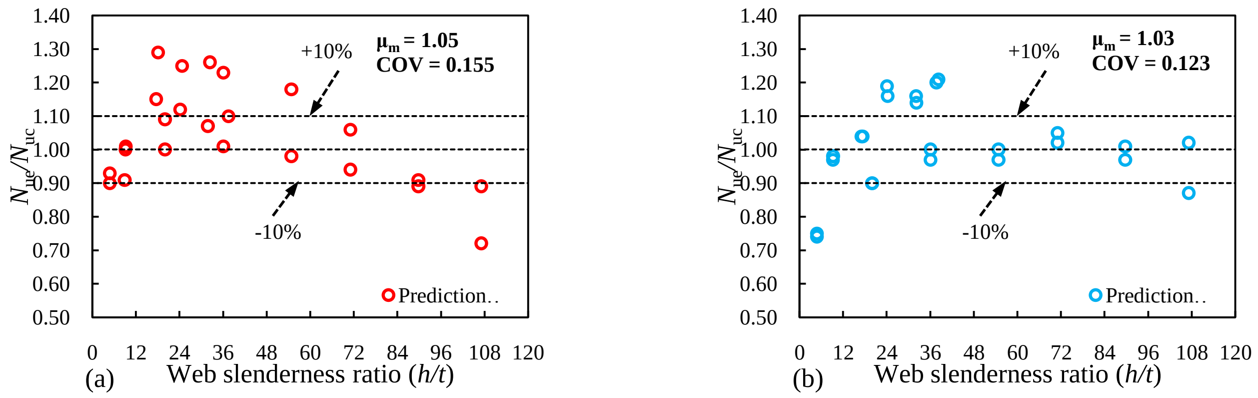

Figure 14.Predicted design strength a) under ETF loading condition for ferritic and b) under ITF loading condition for duplex steel section.

Conditions for different parameters for both types of steel station. For ferritic stainless steel sections the limitations of these parameters are as: $4.8 \leq h/t \leq 107$, $N/t \leq 31$, $N/h \leq 2.6$ and $\theta = 90^o$ and $7.1 \leq h/t \leq 113.6$., $N/t \leq 32.8$, $N/h \leq 2.4$ and $\theta = 90^o$ for the duplex stainless-steel sections.

$$P_p = Ct^2 f_y sin\theta\left(1 - C_R\sqrt{\frac{r_i}{t}}\right)\left(1 + C_N\sqrt{\frac{N}{t}}\right)\left(1 - C_h\sqrt{\frac{h}{t}}\right) + \left[\sigma_{u-ad} . A_{bonding}\right]C_{ad-FRP} \quad (4)$$

where, t is the web thickness; C is the coefficient; f_y is the yield stress of steel section; N is the bearing length; h is the web depth; C_R is the corner radius coefficient (inside); C_N is the bearing length coefficient; C_h is the web slenderness coefficient; σ_{u-ad} is the ultimate tensile stress of adhesives, $A_{bonding}$ is the FRP bonded area and $C_{ad\text{-}FRP}$ is the coefficient of adhesive-FRP.

Table 1. Co-efficient for designed equation under different loading configurations for both types of steel section.

Load cases (Un-fastend)	C_h	C_N	C	C_R	$C_{ad\text{-}FRP}$	LRFD $\emptyset_w$	Section type
E.T.F	0.020	0.490	3.300	0.320	0.025	0.850	Ferritic stainless steel
I.T.F	0.001	0.480	5.400	0.260	0.040	0.850	
E.O.F	0.020	0.450	3.600	0.120	0.040	0.850	
I.O.F	0.010	0.170	10.000	0.230	0.025	0.850	
E.T.F	0.040	0.500	3.500	0.320	0.020	0.800	Lean duplex stainless steel
I.T.F	0.010	0.510	5.500	0.260	0.030	0.850	
E.O.F	0.020	0.490	4.700	0.400	0.035	0.850	
I.O.F	0.020	0.510	7.200	0.400	0.025	0.850	

N_{ue} is the measured ultimate strength of 66 test result and 104 FE results. N_{uc} is the ultimate strength calculated from the proposed design equation (Eq. 4).The predicted ultimate strength was measured for loading conditions ETF and ITF. The overall mean (μ_m) and coefficient of variance (COV) of the ultimate strength for ferric steel under ETF loading condition is 1.05 and 0.155 respectively. The reliability index (β) and resistance factors ($\emptyset_w$) found as 2.52 and 0.85 respectively for ETF loading condition. The prediction accuracy for duplex stainless-steel section is comparatively better than that of ferric stainless-steel section. The values of μ_m and COV are 1.03 and 0.123 respectively. The reliability index (β) and resistance factor for duplex steel section are same as ferric stainless-steel section.

The web crippling design strength for CFRP-strengthened sections were predicted by the proposed design formula and it is showed that the proposed formula is safe and reliable(see Figure 14). The reliability index is higher than the specified values. Consequently, the proposed formula is more reliable and gives consistent results for adhesive-CFRP-strengthened sections for all loading configurations.

8 CONCLUSIONS

Numerical study has been conducted for developing a unique design formula for CFRP strengthened sections for strength of web crippling. The geometrical and material non-linearity has been considered to develop the numerical model. The test results of 66 specimens were taken including the failure modes, web deformation under four different loading conditions. Test results were simulated by developed finite element model. The traction-separation law implemented for analysing debonding between the strengthening materials and steel sections. From the simulated results it is concluded that the web crippling behaviour of the CFRP strengthened sections (SHS and RHS) were predicted properly. Therefore, extensive parametric study has been performed to verify the finite element model for different cross-section and slenderness ratio. Different slenderness ratio was considered that is ranges between 4.7 to 113.6.In case of bridge design, existing design codes for web crippling for CFRP-strengthened stainless steel tubular sections is very conservative. To calculate the ultimate strength accurately under the ETF, ITF, EOF and the ITF loading conditions, a unique design equation was proposed in this paper. Finally, the design guideline is verified with the experimental results and finite element results. Allowable safety margin has been achieved from reliability analysis for web crippling strengths. For both ferric and duplex sections, the proposed guideline for design shows the reliable web crippling strength.

ACKNOWLEDGEMENTS

The authors are thankful to specimen supplying institutions STALA Tube Finland. This research was impossible without the support from The University of Hong Kong. Research facilities and funding from this institution is highly acknowledged.

REFERENCES

ABAQUS. 2009. *ABAQUS analysis user's manual*, version 6.9-1. ABAQUS Inc.

AS. 1991 *Methods for tensile testing of metals*, Australian standard AS 1391. Sydney, Australia: Standards Association of Australia.

ASCE. 2002. ASCE. *Specification for the design of cold-formed stainless-steel structural members*. SEI/ASCE 8-02; Reston, VA: *American Society of Civil Engineers*.

ASTM.1997. *Standard test methods for tension testing of metallic materials*, E 8M-97. West Conshohocken: American Society for Testing and Materials.

Baddoo, N. R. and Burgan, B. A. 2001. Structural design of stainless steel, the steel construction institute, United Kingdom.

Baddoo, N. R. and Kosmac A. 2013. Sustainable duplex stainless-steel bridges, the steel construction institute, United Kingdom.

Fernando D., Yu T., Teng J.G. and Zhao X.L. CFRP strengthening of rectangular steel tubes subjected to end bearing loads: Effect of adhesive properties and finite element modeling. Thin-Walled Structures 2009; 47(10):1020-1028.

Gedge G. 2005. Stainless steel for bridge construction–materials selection for the towers of the stonecutters bridge Hong Kong. In: *International bridge conference*.

Gedge G. 2007. Duplex steels for durable bridge construction. *IABSE Conference*.

Gedge G. 2008. Structural uses of stainless steel — buildings and civil engineering, *Journal of Constructional Steel Research* 64: 1194–1198

Islam S. M.Z, Young B. 2014. FRP strengthening of lean duplex stainless steel hollow sections subjected to web crippling". *Journal of Thin-walled Structures*, 85:183-200.

Islam S.M.Z, Young B. 2015. Use of stainless steel as structural members in bridge construction and fiber reinforced polymer strengthening,". *IABSE-JSCE Joint Conference on Advances in Bridge Engineering-III, 164-173, Dhaka, Bangladesh*

Islam S.M.Z, Yancheng C. and Young B. 2019 "Design of CFRP-strengthened stainless steel tubular sections subjected to web crippling" *Journal of Constructional Steel Research.*159:442-458.

Islam S.M.Z. and Young B. Design of CFRP-Strengthened aluminium tubular sections subjected to web crippling. Thin-Walled Structures, 2018, 124: 605-621.

Islam S.M.Z. Strengthening of aluminium and stainless-steel tubular sections with Fibre-reinforced polymer. PhD Thesis, Department of Civil Engineering, The University of Hong Kong. Hong Kong, China, 2012.

Islam S.M.Z. and Young B. Ferritic stainless-steel tubular members strengthened with high modulus CFRP plate subjected to web crippling. Journal of constructional steel research, 2012; 77:107-18.

Katsuyoshi N, Carol K. Shield, Jerome F. Hajjar 2005. Effective bond length of carbon-fiber-reinforced polymer strips bonded to fatigued steel bridge I-girders, *Journal of Bridge Engineering*, 6(6):514-522.

Miller, T.C., Chajes, M. J., Mertz, D. R. and Hastings, J.N. 2001. Strengthening of a steel bridge girder using CFRP plates. *Journal of Bridge Engineering,* 6(6), 514-522.

Schnerch, D. and Rizkalla, S. 2008. Flexural strengthening of steel bridges with high modulus CFRP strips. *Journal of Bridge Engineering,* 13(2), 192-201.

Sen, R., Liby, L. and Mullins, G. 2001. Strengthening steel bridge sections using CFRP laminates. *Composites Part B: Engineering,* 32(4), 309-322.

Suzuki, H. 2005. First application of carbon fibre reinforced polymer strips to an existing steel bridge in Japan. *Proceedings of the Advanced materials for constructions for bridges, buildings and other structures IV*, Maui, Hawaii.

Tani, K., Matsumura, M., Kitada, T. and Hayashi, H., 2000. Experimental study on seismic retrofitting method of steel bridge piers by using carbon fibre sheets. *Proceedings of the 6th Korea-Japan Joint Seminar on Steel Bridges*, Tokyo, 437-445.

Zhao X. L. and Zhang L. 2007. State-of-the-art review on FRP strengthened steel structures. *Engineering Structures*, 29(8):1808–1823.